Improvement of phase sensitivity in an SU(1,1) interferometer via a phase shift induced by a Kerr medium

Shoukang Chang,[1] Wei Ye,[2] Huan Zhang,[1] Liyun Hu,[1,*] Jiehui Huang,[3,†] and Sanqiu Liu[1,4,‡]
[1]*Center for Quantum Science and Technology, Jiangxi Normal University, Nanchang 330022, China*
[2]*School of Computer Science and Engineering, Central South University, Changsha 410083, China*
[3]*School of Mathematics, Physics and Statistics, Shanghai University of Engineering Science, Shanghai 201620, China*
[4]*Department of Physics, Nanchang University, Nanchang 330031, China*

(Received 23 April 2021; revised 16 September 2021; accepted 14 February 2022; published 3 March 2022)

We theoretically study the phase sensitivity of an SU(1,1) interferometer, in which the phase shift is induced by a Kerr medium, together with a coherent state input and homodyne detection. Considering both ideal and photon-loss cases, the results show that compared with the linear-phase-shift-based SU(1,1) interferometer, the Kerr-phase-shift-based SU(1,1) [KSU(1,1)] interferometer can show the significant enhancement of the phase sensitivity and quantum Fisher information even in the presence of photon losses. In particular, without photon losses, the phase sensitivity of the KSU(1,1) interferometer can break through the standard quantum limit and the Heisenberg limit (HL), even close to the super-HL. From the perspective of quantum resource theory, it is interesting that the phase shift induced by the Kerr medium shows an obvious advantage of low-cost input resources to obtain higher phase sensitivity and larger quantum Fisher information. These findings may have potential applications for state-of-the-art quantum information technology.

DOI: 10.1103/PhysRevA.105.033704

I. INTRODUCTION

Quantum metrology has a close relation to various important information areas, such as Bose-Einstein condensates [1–3], gravitational wave detection [4,5], and quantum imaging [6–8]. It has been widely studied and highly developed in recent years. To meet the high precision demand, all kinds of optical interferometers have been proposed. For instance, as a general model, the Mach-Zehnder interferometer (MZI) has been used as an essential tool to provide insight into tiny variations in phase shift [9–11].

In order to improve precise measurement, generally speaking, we can focus on the following three stages [12]: probe generation [13–16], probe modification [17–21], and probe readout [22,23], as illustrated in Fig. 1(a). In particular, for probe generation, the phase sensitivity is always confined to the standard quantum limit (SQL) when classical resources are injected into the input ports of the MZI. To surpass the SQL, nonclassical quantum states have widely been used as the input of the MZI, such as entangled states [13], twin Fock states [24], and NOON states [25], by which the Heisenberg limit (HL) can even be reached [26,27]. Although the usage of nonclassical states can greatly improve the phase sensitivity of optical interferometers, these states with large average photon numbers are not only more difficult to prepare, but also very fragile especially in the presence of environmental interferences [28–30]. Thus, from the viewpoint of resource theory, it will be a challenging task with a simple input state [such as a coherent state (CS)] to further improve the precision of measurement, especially in the realistic case.

On the other hand, many efforts have been made in the stage of probe modification, especially when Yurke *et al.* first proposed an SU(1,1) interferometer with a linear phase shift [20]. In this system, the active nonlinear optical devices, such as four-wave mixers (FWMs) and optical parametric amplifiers (OPAs), are used instead of the passive linear beam splitters (BSs) used in the conventional MZI [31–37]. To beat the SQL, Plick *et al.* applied strong CS as the input into the SU(1,1) interferometer [33]. Subsequently, Li *et al.* proposed a scheme of reaching HL sensitivity via a squeezed vacuum state (SVS) plus a CS with homodyne detection [31]. It is interesting that Hudelist *et al.* pointed out that the signal-to-noise ratio (SNR) of the SU(1,1) interferometer is about 4.1 dB higher than that of the MZI under the same phase-sensing intensity [38]. This point may be one of reasons for focusing on this interferometer. Actually, this implies the role of a nonlinear process for improving the precision.

In addition to the SU(1,1) nonlinear process, nonlinear phase shifts have also been proposed for enhancing the phase estimation, which can be viewed as another method of probe modification [9,39–42]. For instance, in the traditional MZI, Zhang *et al.* investigated the phase estimation by replacing the linear phase shift with a nonlinear one [9] using a CS and parity measurement. Jiao *et al.* proposed an improved protocol of nonlinear phase estimation by inserting a nonlinear phase shift into the traditional MZI, with active correlation output readout and homodyne detection [39]. More recently, Chang *et al.* suggested a scheme for enhancing phase sensitivity by introducing a nonlinear phase shifter to the modified

*Corresponding author: hlyun@jxnu.edu.cn
†jiehuihuang@126.com
‡sqliu@ncu.edu.cn

 ©2022 American Physical Society

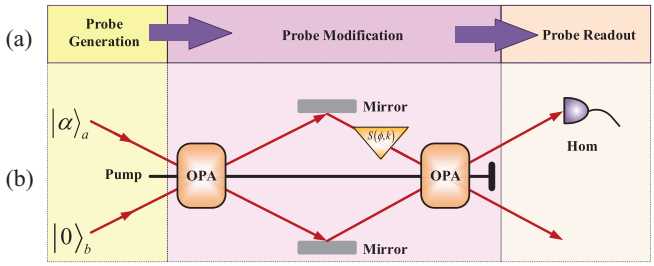

FIG. 1. (a) The general process of estimating an unknown parameter ϕ. (b) Schematic diagram of SU(1,1) interferometer with a nonlinear phase shifter $S(\phi, k)$. The two input ports of this interferometer are a coherent state $|\alpha\rangle_a$ and a vacuum state $|0\rangle_b$, respectively. OPA is an optical parametric amplifier and Hom is a homodyne detection.

interferometer consisting of a balanced BS and an OPA [41]. It is shown that the OPA potential can be stimulated by a nonlinear phase shifter, which is absent for the case of the linear phase shifter. In addition, the estimation of nonlinear phase has also lots of applications, such as the third-order susceptibility of the Kerr medium [39], phase-sensitive amplifiers [43,44], and nonclassical quantum state preparations [45,46]. These results show that nonlinear optical devices can be considered powerful tools to effectively achieve both high accuracy and sensitivity. However, on one hand, the research on nonlinear phase estimation are not as systematic as those on the linear one. On the other hand, most works on phase precision are based on either specific measurement, especially in the presence of photon loss, or direct calculation of quantum Fisher information for an ideal case.

In this paper, we mainly focus on the nonlinear phase estimation of a Kerr-phase-shift-based SU(1,1) [KSU(1,1)] interferometer, together with CS plus vacuum state (VS) (denoted as $|\alpha\rangle_a \otimes |0\rangle_b$) as inputs and homodyne detection. Then, both the phase sensitivity and the quantum Fisher information (QFI) are analytically investigated with and without photon losses. The results show that, without photon losses, the phase sensitivity of the KSU(1,1) interferometer can beat the SQL and the HL, even approaching the super-HL (SHL). Compared to the linear-phase-shift-based SU(1,1) interferometer and other input resources including CS $\otimes$ CS and SVS $\otimes$ CS, the KSU(1,1) interferometer presents much greater QFI and higher phase sensitivity closer to the quantum Cramér-Rao bound (QCRB), even under the photon losses [34,47–50]. From the viewpoint of resource theory, since the CS $\otimes$ VS can be seen as the most simple and easily available input, the KSU(1,1) interferometer scheme has an obvious advantage of low-cost input, compared to other input resources of the SU(1,1) interferometer one.

The remainder of this paper is arranged as follows. In Sec. II, we introduce the phase estimation model in the KSU(1,1) interferometer. In Sec. III, we investigate the phase sensitivity of the output signal with homodyne detection, and then compare them with the conventional SU(1,1) interferometer. In Sec. IV, we derive the QFI of the KSU(1,1) interferometer by invoking the characteristic function (CF) approach. In Sec. V, we mainly consider the effects of photon losses on both phase sensitivity and QFI of the KSU(1,1) interferometer. Finally, conclusions are drawn in the last section.

II. PHASE ESTIMATION MODEL IN KSU(1,1) INTERFEROMETER

Let us begin with the description of the phase estimation model in the KSU(1,1) interferometer, where this interferometer consists of two OPAs (or FWMs) and a Kerr-type medium, as shown in Fig. 1(b). Here we consider a CS $|\alpha\rangle_a$ with $\alpha = |\alpha|e^{i\theta_\alpha}$ and a VS $|0\rangle_b$ as the inputs in mode a and mode b, respectively. Thus the probing state can be shown as $|\psi_{\rm in}\rangle = |\alpha\rangle_a \otimes |0\rangle_b$. After going through the first OPA, the resulting state is given by $\hat{S}(\xi_1)|\psi_{\rm in}\rangle$, i.e., a two-mode squeezed CS, where the operator $\hat{S}(\xi_1) = \exp(\xi_1^* \hat{a}\hat{b} - \xi_1 \hat{a}^\dagger \hat{b}^\dagger)$ represents the OPA process, $\xi_1 = g_1 e^{i\theta_1}$, with a gain factor g_1 and a phase shift θ_1 and $\hat{a}$ ($\hat{a}^\dagger$) and $\hat{b}$ ($\hat{b}^\dagger$) are the annihilation (creation) operators for modes a and b, respectively. For simplicity, we assume that the Kerr-type medium is inset into the path b between the first and second OPAs to generate a nonlinear phase shift ϕ to be estimated.

After the interaction between the state $\hat{S}(\xi_1)|\psi_{\rm in}\rangle$ with the Kerr-type medium, the corresponding modified state becomes

$$|\psi_\phi\rangle = \hat{S}(\phi, k)\hat{S}(\xi_1)|\psi_{\rm in}\rangle, \tag{1}$$

depending on the phase parameter ϕ, where

$$\hat{S}(\phi, k) = e^{i\phi(\hat{b}^\dagger \hat{b})^k} \tag{2}$$

is the nonlinear-phase-shift operator and the exponent k is the order of the nonlinearity. In particular, for the case of $k = 1$, $\hat{S}(\phi, 1) = e^{i\phi \hat{b}^\dagger \hat{b}}$ just reduces to the linear phase shift, while for the case of $k = 2$, $\hat{S}(\phi, 2) = e^{i\phi(\hat{b}^\dagger \hat{b})^2}$ corresponds to Kerr nonlinear case. Throughout this paper, we only consider both Kerr-type nonlinear medium and the linear one by taking $k = 1, 2$, respectively.

After the second OPA, the final output state is given by

$$|\psi_{\rm out}\rangle = \hat{S}(\xi_2)\hat{S}(\phi, k)\hat{S}(\xi_1)|\psi_{\rm in}\rangle, \tag{3}$$

where $\hat{S}(\xi_2) = \exp(\xi_2^* \hat{a}\hat{b} - \xi_2 \hat{a}^\dagger \hat{b}^\dagger)$, with $\xi_2 = g_2 e^{i\theta_2}$, is a two-mode squeezing operator, corresponding to the second OPA process. The Kerr nonlinear phase shifter $\hat{S}(\phi, 2)$ satisfies the transformation relation,

$$\hat{S}^\dagger(\phi, 2)\hat{b}^\dagger \hat{S}(\phi, 2) = e^{-i\phi}\hat{b}^\dagger e^{-i2\phi \hat{b}^\dagger \hat{b}}, \tag{4}$$

which is useful for the calculation of phase sensitivity. One can refer to Appendix A for more details of the derivation for this relation. Finally, the homodyne detection is performed on mode a, so that one can read information about the value of ϕ.

III. PHASE SENSITIVITY VIA HOMODYNE DETECTION

Next, we investigate the phase sensitivity of the KSU(1,1) interferometer. For this purpose, we need to choose a special detection method for the readout of phase information at the final output port. Actually, there are many different detection methods, such as homodyne detection [11,31,32], intensity detection [33,34,47], and parity detection [27,35,36]. Each way of measurement has its own advantages. For example, parity detection has been proven to be an optimal detection for

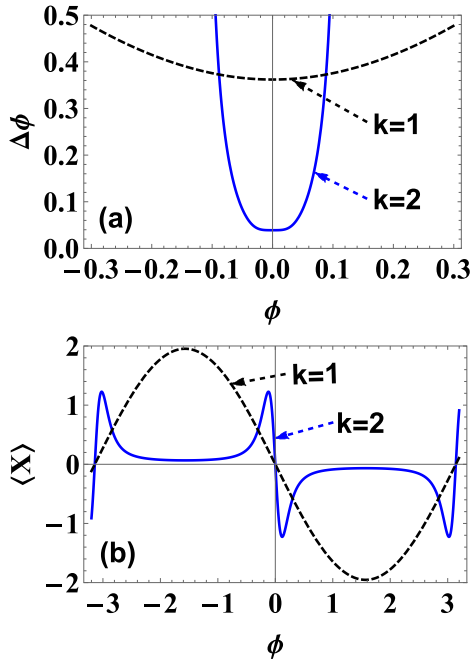

FIG. 2. (a) Phase sensitivity based on homodyne detection and (b) the output signal as a function of ϕ with $g = 1$, $|\alpha| = 1$, and $\theta_\alpha = \frac{\pi}{2}$. The black dashed line and the blue solid line correspond to the linear phase shift ($k = 1$) and the Kerr nonlinear phase shift ($k = 2$), respectively.

linear phase estimation in lots of schemes [27,51]. Compared with both intensity and parity detections, however, homodyne detection can be not only easy to realize with current experimental technology but also simple from the perspective of theoretical calculation, thereby playing a key role in the field of continuous-variable quantum key distribution [52–56]. For this reason, we use the homodyne detection on mode a at one output port to estimate the phase parameter ϕ, where the detected variable is the amplitude quadrature $\hat{X}$, i.e.,

$$\hat{X} = (\hat{a} + \hat{a}^\dagger)/\sqrt{2}. \tag{5}$$

Based on the error propagation formula, the phase sensitivity can be calculated by

$$\Delta\phi = \frac{\sqrt{\Delta^2 \hat{X}}}{|\partial\langle\hat{X}\rangle/\partial\phi|}, \tag{6}$$

with $\Delta^2\hat{X} = \langle\hat{X}^2\rangle - \langle\hat{X}\rangle^2$. According to Eq. (6), for an arbitrary value of ϕ, the corresponding phase sensitivity can be analytically derived. For simplicity, the corresponding expression is not shown here. One can refer to Appendix B for more details. In the following discussions, we assume that the KSU(1,1) interferometer is in a balanced situation, i.e., $\theta_2 - \theta_1 = \pi$ and $g_1 = g_2 = g$.

In Fig. 2(a), we show the phase sensitivity changing with ϕ for the linear ($k = 1$) and nonlinear ($k = 2$) phase shifts when given parameters $g = 1$, $|\alpha| = 1$, and $\theta_\alpha = \pi/2$. It is clearly seen that, for both cases above, the minimum value of the phase sensitivity can be achieved at the optimal point $\phi = 0$. In addition, the phase sensitivity for $k = 2$ is always significantly superior to that for $k = 1$ around the optimal point. This implies that the nonlinear phase shift can be further used to improve the phase sensitivity, compared to the linear one. The reason lies in that the nonlinear phase shift can increase the slope $\partial\langle\hat{X}\rangle/\partial\phi$ of the output signal $\langle\hat{X}\rangle$ at $\phi = 0$, which leads to the increase of the denominator in Eq. (6), as shown in Fig. 2(b). In fact, this point will be clear by deriving the phase sensitivity $\Delta\phi_k$ for $k = 1, 2$ at $\phi = 0$, which is given by

$$\Delta\phi_1 = \frac{1}{\sqrt{N_\alpha} N_{\rm OPA}}, \tag{7}$$

$$\Delta\phi_2 = \frac{\Delta\phi_1}{1 + N_{\rm OPA}(N_\alpha + 2)}, \tag{8}$$

where $\Delta\phi_1$ represents the phase sensitivity of the traditional SU(1,1) interferometer with a linear phase shift $k = 1$, $N_\alpha = |\alpha|^2$ is the mean photon number of the input coherent state, and $N_{\rm OPA} = 2\sinh^2 g$ is the total photon number after the first OPA with vacuum inputs. Obviously, $\Delta\phi_2 < \Delta\phi_1$.

Moreover, from Fig. 2(b) it is shown that the peak width for the case of $k = 2$ is narrower than that for the case of $k = 1$. In this sense, the nonlinear phase shift can also improve superresolution compared to the linear one. On the other hand, to display the effects of both the coherence amplitude $|\alpha|$ and the gain factor g on the phase sensitivity, at the optimal point $\phi = 0$, we also plot the phase sensitivity as a function of $|\alpha|$ and g with different values of $k = 1, 2$, in Figs. 3(a) and 3(b), respectively. It is found that the values of $\Delta\phi$ rapidly decrease with the increase of $|\alpha|$ and g, especially for the case of $k = 2$.

To further show the advantage of the KSU(1,1) interferometer, we also make a comparison about phase sensitivities, involving the SQL ($\Delta\phi \sim 1/\sqrt{N_{\rm Total}}$), the HL ($\Delta\phi \sim 1/N_{\rm Total}$), and the SHL ($\Delta\phi \sim 1/N_{\rm Total}^2$), as shown in Fig. 4. Note that $N_{\rm Total} = \langle\psi_{\rm in}|\hat{S}^\dagger(\xi_1)(\hat{a}^\dagger\hat{a} + \hat{b}^\dagger\hat{b})\hat{S}(\xi_1)|\psi_{\rm in}\rangle$ is the total mean photon number inside the KSU(1,1) interferometer. From Fig. 4, the black dashed line is the sensitivity performance of the linear phase shift, which can only break through SQL and is always surpassed by that of the Kerr nonlinear phase shift. In particular, the latter can break both the SQL and the HL, but cannot beat the SHL. The reason may be that adopting the Kerr nonlinear phase shift to effectively improve the maximum amount of information about the unknown phase shift ϕ can result in a transition from HL ($\Delta\phi \sim 1/N_{\rm Total}$) to SHL ($\Delta\phi \sim 1/N_{\rm Total}^2$), as described in Refs. [9,57–62]. Nevertheless, the common feature of these two is that the phase sensitivity increases with the increase of $|\alpha|$ and g.

In addition, we make a comparison about the performance of phase sensitivity. In Fig. 5, the phase sensitivity is plotted as a function of the total average input photon number N with several different input resources, including $|\alpha\rangle_a \otimes |\beta\rangle_b$, $|\alpha\rangle_a \otimes |\varsigma, 0\rangle_b$ and $|\alpha\rangle_a \otimes |0\rangle_b$ used in the traditional SU(1,1) interferometer ($k = 1$) and $|\alpha\rangle_a \otimes |0\rangle_b$ used in the KSU(1,1) interferometer ($k = 2$). It is shown that, for the traditional case, the phase sensitivity with the input $|\alpha\rangle_a \otimes |0\rangle_b$ performs the worst among these three inputs [31,32]. This implies that the introduction of coherence amplitude $|\alpha|$ or squeezing parameter ς is beneficial for the phase sensitivity improvement. Particularly, it is interesting that, compared to those input states of the traditional SU(1,1) interferometer, the higher phase sensitivity can be achieved only using the

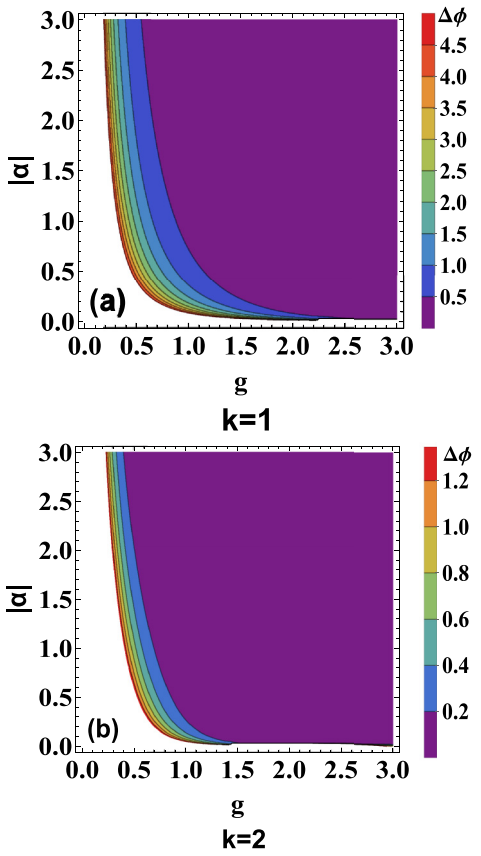

FIG. 3. Phase sensitivity based on homodyne detection as a function of the gain factor g and the coherent amplitude $|\alpha|$ with $\theta_\alpha = \pi/2$ and $\phi = 0$ for (a) the linear phase shift ($k = 1$) and (b) the Kerr nonlinear phase shift ($k = 2$), respectively.

simplest input $|\alpha\rangle_a \otimes |0\rangle_b$ in the KSU(1,1) interferometer. That is to say, for a simple input with less energy and less resources, the phase sensitivity can be further improved by the Kerr-medium-induced phase shift.

IV. THE QFI IN THE KSU(1,1) INTERFEROMETER

As an elegant approach, the QFI can be used to visually describe the maximum amount of information about the unknown phase shift ϕ, which is connected with the QCRB. In fact, the QFI is the intrinsic information in a quantum state and is independent of any specific detection scheme. In the absence of losses, for a pure state, the corresponding QFI can be calculated as [34,48,49]

$$F = 4[\langle\psi'_\phi|\psi'_\phi\rangle - |\langle\psi'_\phi|\psi_\phi\rangle|^2], \tag{9}$$

where $|\psi_\phi\rangle = \hat{S}(\phi, k)\hat{S}(\xi_1)|\psi_{\rm in}\rangle$ is the state vector prior to the second OPA and $|\psi'_\phi\rangle = \partial|\psi_\phi\rangle/\partial\phi$. Then, for the linear phase shift ($k = 1$) and the Kerr nonlinear phase shift ($k = 2$), the QFI can be, respectively, given by [45]

$$F_1 = 4\langle\Delta^2\hat{n}\rangle, \quad F_2 = 4\langle\Delta^2\hat{n}^2\rangle, \tag{10}$$

where $\hat{n} = \hat{b}^\dagger\hat{b}$ is the photon number operator on mode b and $\langle\Delta^2\hat{n}^j\rangle = \langle\bar{\psi}_{\rm out}|(\hat{n}^j)^2|\bar{\psi}_{\rm out}\rangle - \langle\bar{\psi}_{\rm out}|\hat{n}^j|\bar{\psi}_{\rm out}\rangle^2$ ($j = 1, 2$) with the state vector after the first OPA, i.e., $|\bar{\psi}_{\rm out}\rangle = \hat{S}(\xi_1)|\psi_{\rm in}\rangle$.

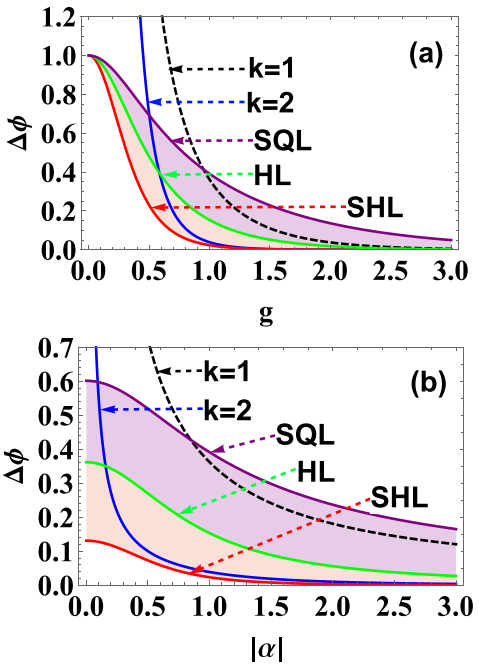

FIG. 4. Phase sensitivity based on homodyne detection as a function of (a) the gain factor g with $|\alpha| = 1$ and (b) the coherent amplitude $|\alpha|$ with $g = 1$ ($\theta_\alpha = \pi/2$). The black dashed and blue solid lines are respectively the linear phase shift ($k = 1$) and the Kerr nonlinear phase shift ($k = 2$), while the purple, green, and red solid lines respectively correspond to the SQL, HL, and SHL.

Using the normal ordering forms of the operators,

$$(\hat{b}^\dagger\hat{b})^4 = \hat{b}^{\dagger4}\hat{b}^4 + 6\hat{b}^{\dagger3}\hat{b}^3 + 7\hat{b}^{\dagger2}\hat{b}^2 + \hat{b}^\dagger\hat{b},$$
$$(\hat{b}^\dagger\hat{b})^2 = \hat{b}^{\dagger2}\hat{b}^2 + \hat{b}^\dagger\hat{b}, \tag{11}$$

and the characteristic function method for calculating average, we have

$$F_1 = 4\big(\bar{A}_2 + \bar{A}_1 - \bar{A}_1^2\big), \quad F_2 = F_1 + f, \tag{12}$$

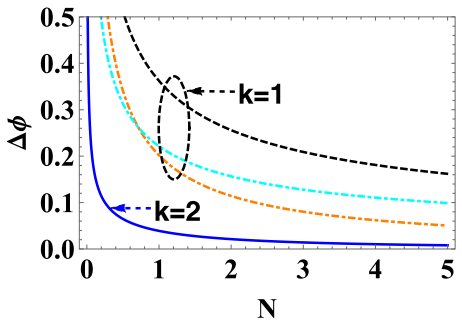

FIG. 5. Phase sensitivity based on homodyne detection as a function of the total average photon number N of input state with $g = 1$. The orange and cyan dot-dashed lines respectively correspond to SVS ⊗ CS and CS ⊗ CS as the inputs with the linear phase shift ($k = 1$), as shown in Refs. [31,32], while the black dashed and blue solid lines are CS ⊗ VS as the input with the linear phase shift ($k = 1$) and the Kerr nonlinear phase shift ($k = 2$), respectively.

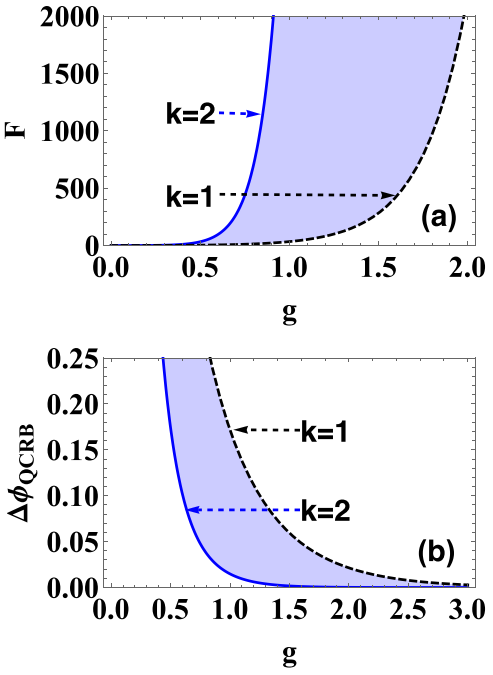

FIG. 6. (a) The quantum Fisher information F and (b) the QCRB as a function of gain factor g for $|\alpha| = 1$ ($\theta_\alpha = \pi/2$), respectively. The black dashed and blue solid lines correspond to linear phase shift ($k = 1$) and Kerr nonlinear phase shift ($k = 2$), respectively.

with

$$f = 4[\bar{A}_4 + 6(\bar{A}_3 + \bar{A}_2) - \bar{A}_2(\bar{A}_2 + 2\bar{A}_1)], \tag{13}$$

$$\bar{A}_m = m!(\sinh^{2m} g)L_m(-|\alpha|^2), \quad m \in \{1, 2, 3, 4\}, \tag{14}$$

and $L_m(\bullet)$ are the Laguerre polynomials. One can refer to Appendix C for more details about derivations of $\bar{A}_m$. Based on Eq. (12), we can give the QCRB $\Delta\phi_{\rm QCRB}$, which represents the lower bound of the phase sensitivity, i.e.,

$$\Delta\phi_{\rm QCRB} = \frac{1}{\sqrt{\upsilon F_k}} \ (k = 1, 2), \tag{15}$$

where υ is the number of trials. For simplicity, here we set $\upsilon = 1$. In general, the smaller the values of $\Delta\phi_{\rm QCRB}$, the higher the phase sensitivity.

To clearly see this point, according to Eqs. (12) and (15), at a fixed $|\alpha| = 1$, Fig. 6 shows the QFI and the QCRB changing with g for different $k = 1, 2$. It is clear that, for the cases of $k = 1, 2$, the values of the QFI increase significantly with the increase of g, thereby leading to more precise phase sensitivity. Moreover, when given the same gain factor g, both the QFI and the QCRB of $k = 2$ always outperform those of $k = 1$, which distinctly shows the superiority of the nonlinear phase shift compared to the linear case. This result originates from the additional item f in Eq. (12), giving rise to the increase of QFI.

As a comparison, we also consider the $\Delta\phi_{\rm QCRB}$ as a function of N for several different input resources in Fig. 7, similar to the phase sensitivity (in Fig. 5). Some similar results are obtained. For instance, although the QCRB with $|\alpha\rangle_a \otimes |0\rangle_b$ is worse than that with other resources in the traditional SU(1,1) interferometer [63], the smallest value of $\Delta\phi_{\rm QCRB}$ can be realized by using $|\alpha\rangle_a \otimes |0\rangle_b$ as the input of the KSU(1,1) interferometer. In addition, from Figs. 5 and 7, it is found that, compared with several different input resources in the traditional SU(1,1) interferometer, the simple input $|\alpha\rangle_a \otimes |0\rangle_b$ of the KSU(1,1) interferometer is closer to the ultimate phase precision $\Delta\phi_{\rm QCRB}$.

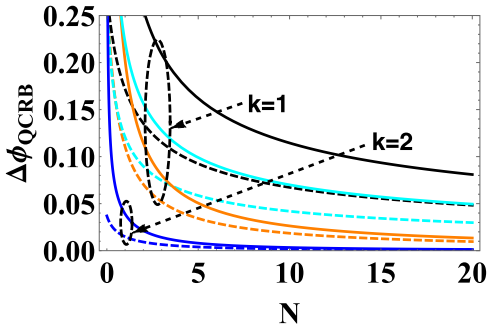

FIG. 7. The $\Delta\phi_{\rm QCRB}$ as a function of the total average photon number N of input state with $g = 1$. The orange and cyan lines respectively correspond to SVS $\otimes$ CS and CS $\otimes$ CS as the inputs with the linear phase shift ($k = 1$), while the black and blue lines correspond to CS $\otimes$ VS as the input with the linear phase shift ($k = 1$) and the Kerr nonlinear phase shift ($k = 2$), respectively. The dashed and solid lines correspond to the $\Delta\phi_{\rm QCRB}$ and the $\Delta\phi$, respectively.

V. THE EFFECTS OF PHOTON LOSSES

In the realistic scenario, there always exists the interaction between the interferometer system and its surrounding environment, e.g., in the presence of photon losses, the information leakage from the system to the environment. For this reason, the system performance would drop severely. In general, there are many types of interactions with the environment on the interferometer [64,65], such as photon loss, imperfect visibility, phase diffusion, and so on. Here, for simplicity, we only study the effects of photon losses on both the phase sensitivity and the QFI in the KSU(1,1) interferometer.

A. The effects of photon losses on the phase sensitivity

First, let us consider the effects of photon losses on the phase sensitivity of the KSU(1,1) interferometer. The Kerr interaction can be described by the Hamiltonian, i.e., $\omega(\hat{b}^\dagger\hat{b})^2$. Thus when considering both the nonlinear effect and photon losses, the density operator satisfies the following master equation, i.e.,

$$\frac{d\hat{\rho}}{dt} = -i\omega[(\hat{b}^\dagger\hat{b})^2, \hat{\rho}] + 2\gamma\hat{b}\hat{\rho}\hat{b}^\dagger - \gamma\hat{b}^\dagger\hat{b}\hat{\rho} - \gamma\hat{\rho}\hat{b}^\dagger\hat{b}, \tag{16}$$

where γ is the loss-rate parameter and $\omega = -\phi/t$ is the third-order nonlinear susceptibility $\chi^{(3)}$, with t being the time for the light to cross the Kerr-type medium [9,66,67].

Upon rescaling the quantities with respect to the loss parameter γ,

$$\tau = \gamma t, \ \tilde{\omega} = -\omega/\gamma, \tag{17}$$

we can rewrite Eq. (16) as

$$\frac{d\hat{\rho}}{d\tau} = i\tilde{\omega}[(\hat{b}^\dagger\hat{b})^2, \hat{\rho}] + 2\hat{b}\hat{\rho}\hat{b}^\dagger - \hat{b}^\dagger\hat{b}\hat{\rho} - \hat{\rho}\hat{b}^\dagger\hat{b}. \tag{18}$$

Under the representation of Fock states, the solution for the master equation can be calculated as

$$\hat{\rho}(\tau) = \sum_{m,n,l=0}^{\infty} C^2_{m,n,l}\hat{\rho}_{0,m+l,n+l}|m\rangle\langle n|, \tag{19}$$

where $\hat{\rho}_{0,m+l,n+l} = \langle m+l|\hat{\rho}_0|n+l\rangle$ is the matrix element of the initial state $\hat{\rho}_0$ and

$$C^2_{m,n,l} = \sqrt{\frac{(n+l)!(m+l)!}{n!m!}}\frac{\Lambda^l}{l!}e^{i\tilde{\omega}\tau(m^2-n^2)-\tau(m+n)}, \tag{20}$$

$$\Lambda = \frac{\tau(1-e^{-2(\tau-i\tilde{\omega}\tau(m-n))})}{\tau - i\tilde{\omega}\tau(m-n)}. \tag{21}$$

One can refer to Appendix D for more details of the derivation for this solution in Eq. (19). For the KSU(1,1) interferometer scheme, when the initial state is $\hat{\rho}_0 = \hat{S}(\xi_1)|\psi_{\text{in}}\rangle\langle\psi_{\text{in}}|\hat{S}^\dagger(\xi_1)$ after the first OPA, the corresponding matrix element can be expressed as

$$\begin{aligned}\hat{\rho}_{0,m+l,n+l} = {} & N_{m,n,l}(\hat{a}^\dagger)^{m+l}\exp(\hat{a}^\dagger\alpha\,\text{sech}g)|0\rangle \\ & \times\langle 0|\exp(\hat{a}\alpha^*\,\text{sech}g)\hat{a}^{n+l},\end{aligned} \tag{22}$$

where

$$N_{m,n,l} = \frac{e^{-|\alpha|^2}(-\tanh g)^{m+n+2l}\text{sech}^2 g}{\sqrt{(m+l)!(n+l)!}}.$$

By substituting Eq. (22) into Eq. (19), one can finally obtain the evolution of the density operator $\hat{\rho}(\tau)$ over the photon-loss channel. After undergoing the second OPA, the density operator of output states can be further given by

$$\hat{\rho}_{\text{out}}(\tau) = \hat{S}(\xi_2)\hat{\rho}(\tau)\hat{S}^\dagger(\xi_2). \tag{23}$$

Based on Eq. (23), it is not difficult to obtain the phase sensitivity $\Delta\phi_{L_2}$ under the case of losses (not shown here for simplicity). In particular, at the optimal point $\phi = 0$, for the KSU(1,1) interferometer in the presence of photon loss, the phase sensitivity $\Delta\phi_{L_2}$ is derived as

$$\Delta\phi_{L_2} = \frac{\sqrt{2(\cosh^2 g - e^{-\tau}\sinh^2 g)^2 - 1}}{2|\text{Re}(\partial\Theta_{n,l}/\partial\phi|_{\phi=0})|\sinh g}, \tag{24}$$

where we have set

$$\begin{aligned}\Theta_{n,l} = {} & e^{-|\alpha|^2}\text{sech}^2 g\sum_{n,l=0}^{\infty}\frac{\varepsilon^l}{l!n!}e^{-(\tau-i\phi)(2n+1)} \\ & \times(-\tanh g)^{2n+2l+1}\Upsilon_{n,l},\end{aligned} \tag{25}$$

with

$$\begin{aligned}\varepsilon &= \frac{\tau(1-e^{-2(\tau-i\phi)})}{\tau - i\phi}, \\ \epsilon_1 &= s + \alpha^*\text{sech}g, \\ \epsilon_2 &= f + \alpha\text{sech}g, \\ \Upsilon_{n,l} &= \frac{\partial^{2n+2l+1}}{\partial s^{n+l}\partial f^{n+l+1}}\exp(\epsilon_1\epsilon_2)|_{s=f=0}.\end{aligned} \tag{26}$$

Note that for the traditional SU(1,1) interferometer in the presence of photon losses, one can refer to Appendix D for more details.

In order to visually see the differences between the photon losses and the ideal cases, at fixed values of the gain factor $g = 1$ and the rescaled time $\tau = 0.4$, we plot the phase sensitivity $\Delta\phi_{L_k}$ $(k = 1, 2)$ as a function of the total average input photon number N, as shown in Fig. 8(a). It is shown that, for the case of $k = 1$, the gap with $|\alpha\rangle_a \otimes |\beta\rangle_b$ (cyan lines) rather than other input resources, between the ideal and loss cases, is relatively smaller, which means that the two CS inputs are more robust against photon losses. In addition, the worst performance is still kept by using CS ⊗ VS as the input of the traditional SU(1,1) interferometer. However, the best performance of phase sensitivity (blue lines) can be achieved by using the CS ⊗ VS as the input of the KSU(1,1) interferometer, even in the presence of photon losses.

Further, we also consider the effects of the rescaled time τ on phase sensitivity $\Delta\phi_{L_k}$ $(k = 1, 2)$ for several different input resources, involving CS ⊗ SVS, CS ⊗ CS, and CS ⊗ VS, when given some values $g = 1$ and $N = 10$, as shown in Fig. 8(b). It is clear that for $k = 1, 2$, the value of $\Delta\phi_{L_k}$ increases with the increase of τ, which shows that the phase sensitivity can be deeply influenced by the photon losses. Even so, the value of $\Delta\phi_{L_k}$ for $k = 2$ with $|\alpha\rangle_a \otimes |0\rangle_b$ is smaller than that for $k = 1$ with inputting $|\alpha\rangle_a \otimes |\beta\rangle_b$ (or $|\alpha\rangle_a \otimes |\varsigma, 0\rangle_b$), and then increases much more slowly with the increase of τ. These results above imply that the phase sensitivity of $k = 2$ with $|\alpha\rangle_a \otimes |0\rangle_b$ is more robust against photon losses.

B. The effects of photon losses on the QFI

For a realistic case, the output state after a lossy channel is usually a mixed state rather than a pure one. Thus the QFI cannot be directly discussed according to Eq. (6). In this situation, one may appeal to the spectral decompositions of density operator [68,69]. Rossi *et al.* used this method to study the characterization of dissipative bosonic channels and showed that the introduction of Kerr nonlinearity can enhance estimation of the loss rate by Gaussian probes (coherent or squeezed) [70,71]. Generally speaking, this method is difficult not only to obtain the spectral decompositions, but also to derive the analytical expression of the QFI. Fortunately, Escher *et al.* proposed a way to obtain an upper bound to the QFI in the presence of photon losses [72]. The basic idea is to purify the whole system involving an initial pure state and an environment by introducing additional degrees of freedom, so that the present problem is converted to the parameter estimation under a unitary evolution $\hat{U}_{S+E}(\phi)$. We use this way to obtain the analytical QFI in a realistic case. For this purpose, we first make a brief review in the following.

Given an initial pure state $|\psi_S\rangle$ in the probe system S and an initial state $|0_E\rangle$ in the environment, the purified state $|\psi_{S+E}\rangle$ in the enlarged space can be given by

$$\begin{aligned}|\psi_{S+E}\rangle &= \hat{U}_{S+E}(\phi)|\psi_S\rangle|0_E\rangle \\ &= \sum_{l=0}^{\infty}\hat{\Pi}_l(\phi)|\psi_S\rangle|l_E\rangle,\end{aligned} \tag{27}$$

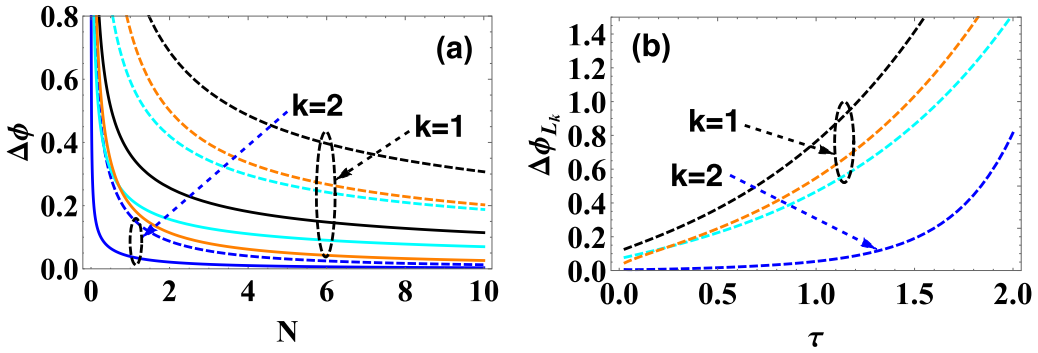

FIG. 8. Phase sensitivity based on homodyne detection as a function of (a) the total average photon number N of the input state with $g = 1$, $\tau = 0.4$, and of (b) the rescaled time τ with $g = 1$, $N = 10$ ($\theta_\alpha = \pi/2$). The orange and cyan lines respectively correspond to SVS $\otimes$ CS and CS $\otimes$ CS as the inputs with the linear phase shift ($k = 1$), while the black and blue lines correspond to CS $\otimes$ VS as the input with the linear phase shift ($k = 1$) and the Kerr nonlinear phase shift ($k = 2$), respectively. The dashed and solid lines correspond to photon losses and no photon losses, respectively.

where $\hat{\Pi}_l(\phi)$ is the Kraus operator describing the photon losses (also including the effect of phase shift), and $|l_E\rangle$ is an orthogonal basis of the state $|0_E\rangle$. In this situation, for the whole purified system, the QFI $C_Q[|\psi_S\rangle, \hat{\Pi}_l(\phi)]$ turns out to be

$$C_Q[|\psi_S\rangle, \hat{\Pi}_l(\phi)] = 4[\langle\psi'_{S+E}|\psi'_{S+E}\rangle - |\langle\psi'_{S+E}|\psi_{S+E}\rangle|^2]. \tag{28}$$

According to Eqs. (27) and (28), the upper bound $C_Q[|\psi_S\rangle, \hat{\Pi}_l(\phi)]$ can be given in terms of Kraus operators,

$$C_Q[|\psi_S\rangle, \hat{\Pi}_l(\phi)] = 4\big[\langle\hat{H}_1(\phi)\rangle_S - \langle\hat{H}_2(\phi)\rangle_S^2\big], \tag{29}$$

with the averages $\langle\cdot\rangle_S$ being derived in $|\psi_S\rangle$ and

$$\hat{H}_1 = \sum_{l=0}^{\infty} \frac{d\hat{\Pi}_l^\dagger(\phi)}{d\phi}\frac{d\hat{\Pi}_l(\phi)}{d\phi}, \tag{30}$$

$$\hat{H}_2 = i\sum_{l=0}^{\infty} \frac{d\hat{\Pi}_l^\dagger(\phi)}{d\phi}\hat{\Pi}_l(\phi). \tag{31}$$

Actually, Eq. (29) provides an upper bound to the QFI $F_L \leqslant C_Q[|\psi_S\rangle, \hat{\Pi}_l(\phi)]$ for the reduced system [62]; thus one needs to find the minimal value over all Kraus operators $\{\Pi_l(\phi)\}$, i.e.,

$$F_L = \min_{\{\Pi_l(\phi)\}} C_Q[|\psi_S\rangle, \hat{\Pi}_l(\phi)]. \tag{32}$$

Next, we consider the QFI of the KSU(1,1) scheme with the photon losses placed before or after the Kerr nonlinear phase shift in the b arm, as shown in Fig. 9. The corresponding Kraus operator $\hat{\Pi}_l(\phi)$ including the nonlinear phase can be written as the general form

$$\hat{\Pi}_l(\phi) = \sqrt{\frac{(1-\eta)^l}{l!}}e^{i\phi[(\hat{b}^\dagger\hat{b})^2 - 2\mu_1\hat{b}^\dagger\hat{b}l - \mu_2 l^2]}\eta^{\frac{\hat{n}}{2}}\hat{b}^l, \tag{33}$$

where η denotes the strength of the photon loss. $\eta = 0$ and $\eta = 1$ describe the complete absorption and lossless cases, respectively. μ_1 and μ_2 are two variational parameters with $\mu_1 = \mu_2 = 0$ and $\mu_1 = \mu_2 = -1$ corresponding to the photon losses occurring before and after the Kerr nonlinear phase shift, respectively.

To derive Eq. (29) using Eq. (33), we adopt the technique of integration within an ordered product of operators (IWOP) [73] to obtain the operator identity (see Appendix E), i.e.,

$$\eta^{\hat{n}}\hat{n}^q =: \frac{\partial^q}{\partial x^q}e^{(\eta e^x - 1)\hat{b}^\dagger\hat{b}}\Big|_{x=0} :, \tag{34}$$

where $:\cdot:$ indicates the symbol of the normal ordering form, which further leads to the formula (see Appendix E)

$$\sum_{l=0}^{\infty}\frac{(1-\eta)^l}{l!}l^p\hat{b}^{\dagger l}\eta^{\hat{n}}\hat{n}^q\hat{b}^l = D_{q,p}[\eta e^x + (1-\eta)e^y]^{\hat{b}^\dagger\hat{b}}, \tag{35}$$

with $D_{q,p} = \frac{\partial^{q+p}}{\partial x^q\partial y^p}[\cdot]_{|x=y=0}$ being a partial differential operator.

Using Eq. (35) and the following transformation relations,

$$\begin{aligned} e^{\lambda\hat{b}^\dagger\hat{b}}\hat{b}^l e^{-\lambda\hat{b}^\dagger\hat{b}} &= e^{-\lambda l}\hat{b}^l, \\ e^{\lambda(\hat{b}^\dagger\hat{b})^2}\hat{b}^l e^{-\lambda(\hat{b}^\dagger\hat{b})^2} &= e^{\lambda l^2}\hat{b}^l e^{-2\lambda l\hat{b}^\dagger\hat{b}}, \end{aligned} \tag{36}$$

the upper bound of the QFI $C_Q[|\psi_S\rangle, \hat{\Pi}_l(\phi)]$ can be calculated as (see Appendix F)

$$\begin{aligned} C_Q[|\psi_S\rangle, \hat{\Pi}_l(\phi)] =& 4(W_1^2\langle\Delta^2\hat{n}^2\rangle - W_2\langle\hat{n}^3\rangle + W_3\langle\hat{n}^2\rangle \\ &- W_4\langle\hat{n}\rangle - W_5\langle\hat{n}^2\rangle\langle\hat{n}\rangle - W_6\langle\hat{n}\rangle^2), \end{aligned} \tag{37}$$

where $\langle\cdot\rangle$ and $\langle\Delta^2\cdot\rangle$ are, respectively, the average and variance under the state $|\psi_S\rangle$, where $|\psi_S\rangle = S(\xi_1)|\psi_{\text{in}}\rangle$ is the state vector after the first OPA. W_j ($j = 1, 2, 3, 4, 5, 6$) are given in Appendix E and not shown here, for simplicity. In particular, when $C_Q[|\psi_S\rangle, \hat{\Pi}_l(\phi)]$ reaches the minimum value

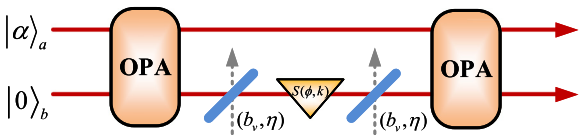

FIG. 9. Schematic diagram of the photon losses that occur before and after the nonlinear phase. η is the transmissivity of the fictitious BS; b_v is the vacuum operator.

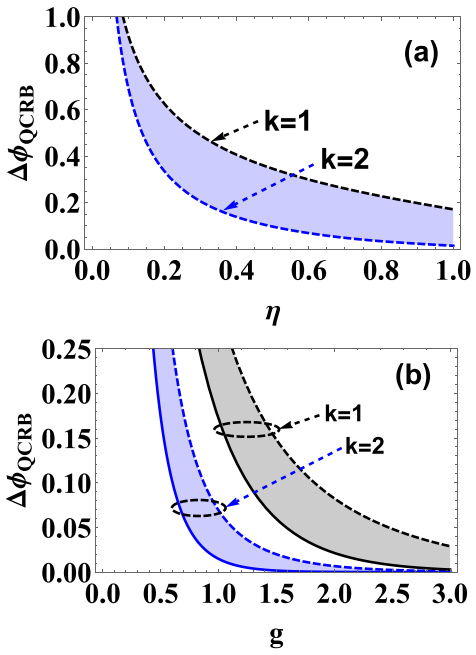

FIG. 10. The $\Delta\phi_{\mathrm{QCRB}}$ as a function of (a) the transmissivity η with $g = 1$ and $|\alpha| = 1$, and (b) the gain factor g with $|\alpha| = 1$. The black and blue lines correspond to $k = 1, 2$, and the dashed and solid lines correspond to the effects of photon losses and no photon losses, respectively.

corresponding to the QFI F_L, the variational parameters μ_1 and μ_2 are, respectively, given by

$$\mu_{1\mathrm{opt}} = \frac{BE - CD}{AD - 2\eta B^2}, \tag{38}$$

$$\mu_{2\mathrm{opt}} = \frac{AE - 2\eta BC}{AD - 2\eta B^2}, \tag{39}$$

where A, B, C, D, and E are shown in Appendix E. Upon substituting those optimal results $\mu_{1\mathrm{opt}}$ and $\mu_{2\mathrm{opt}}$ into C_Q, the minimum value of C_Q, i.e., the QFI F_L of the Kerr nonlinear phase shift in the presence of photon losses, can be derived theoretically.

Considering a CS and a VS input, here we numerically analyze the QCRB $\Delta\phi_{\mathrm{QCRB}}$ which actually is equivalent to the QFI due to the relation in Eq. (15). For fixed parameters with $|\alpha| = 1$ and $\theta_\alpha = \pi/2$, the QCRB $\Delta\phi_{\mathrm{QCRB}}$ as a function of transmissivity η and gain factor g are shown in Fig. 10. As a comparison, the linear case with $k = 1$ is also plotted here. It is clear that the bound performance of phase sensitivity becomes better and better with the increase of both transmissivity η and gain factor g for $k = 1, 2$ [see the dashed lines in Figs. 10(a) and 10(b)]. The QCRB for $k = 2$ always outperforms that for $k = 1$, and the gap between them first increases and then decreases with the increase of η and g. Compared to the ideal cases [solid lines in Fig. 10(b)], it is clear that photon losses present an obvious effect on the QCRB [dashed lines in Fig. 10(b)]. However, it is interesting that the gap of QCRB for $k = 2$ between ideal and nonideal cases is significantly smaller than that for $k = 1$, which is also going to be smaller with the increase of g especially for $k = 2$. Again, this implies that the combination of Kerr nonlinearity and OPA can further reduce the influence of photon losses on the QFI.

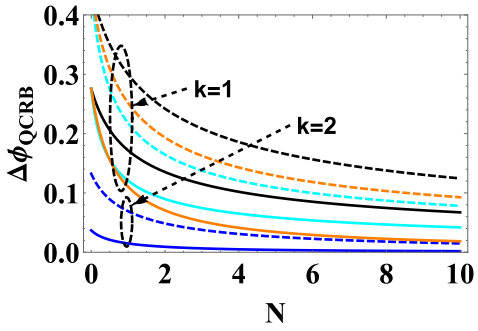

FIG. 11. The $\Delta\phi_{\mathrm{QCRB}}$ as a function of the total average photon number N of the input state with $g = 1$, $\eta = 0.6$. The orange dashed and cyan dashed lines respectively correspond to SVS $\otimes$ CS and CS $\otimes$ CS as the inputs with the linear phase shift ($k = 1$), as shown in Ref. [63]. The black and blue lines correspond to CS $\otimes$ VS as the input with the linear phase shift ($k = 1$) and the Kerr nonlinear phase shift ($k = 2$), respectively. The dashed and solid lines correspond to the effects of photon losses and no photon losses, respectively.

In addition, under the photon-loss processes (e.g., $\eta = 0.6$), we further consider the $\Delta\phi_{\mathrm{QCRB}}$ as a function of total average input photon number N for those different input resources above, when given parameter $g = 1$, as shown in Fig. 11. Here the solid lines correspond to the ideal cases for a comparison. It is clearly seen that, compared to other input resources, the input $|\alpha\rangle_a \otimes |0\rangle_b$ of the traditional SU(1,1) interferometer has larger values of the QCRB with and without photon losses, but for the KSU(1,1) interferometer, the input $|\alpha\rangle_a \otimes |0\rangle_b$ is always smaller values of the QCRB even in the nonideal case. This means that the KSU(1,1) interferometer with and without photon losses shows an obvious advantage of low-cost input resources to obtain a better QCRB.

VI. CONCLUSIONS

In summary, we have investigated the phase estimation of the KSU(1,1) interferometer, accompanied with $|\alpha\rangle_a \otimes |0\rangle_b$ and homodyne detection. One of the major innovations presented in this paper is that, by using the CF method and the IWOP technique, the analytical expression of the QFI is derived in both ideal and unideal scenarios. It is shown that the increase of both gain factor g and coherent amplitude $|\alpha|$ is beneficial for improving both the phase sensitivity and the QCRB. Compared to the linear-phase-shift-based SU(1,1) interferometer, the KSU(1,1) interferometer presents a significantly better performance about both of them, especially around the optimal point $\phi = 0$. In particular, for the ideal case, the KSU(1,1) interferometer at the large g and $|\alpha|$ levels beats both the SQL and the HL, even approaching the SHL. In addition, we investigate the effects of the photon losses on the phase sensitivity by invoking the master equation. It is found that the KSU(1,1) interferometer with inputting simple resources CS $\otimes$ VS still provides a significant improvement for the phase estimation in contrast to the linear-phase-shift-based SU(1,1) interferometer in the presence of photon losses.

To further show the advantages of the KSU(1,1) interferometer, with and without photon losses, we also evaluate the QCRB changing with total average input photon number N for several different input resources, including $|\alpha\rangle_a \otimes |0\rangle_b$, $|\alpha\rangle_a \otimes |\beta\rangle_b$, and $|\alpha\rangle_a \otimes |\varsigma, 0\rangle_b$, when given a parameter $g = 1$. It is found that the best performance can be achieved only using the simplest input $|\alpha\rangle_a \otimes |0\rangle_b$ in the KSU(1,1) interferometer, which is significantly superior to those input resources in the traditional SU(1,1) interferometer. This means that, for a simple input with less energy and less resources, the KSU(1,1) interferometer also presents larger QFI. Finally, we should mention that the QFI in the presence of photon losses can be enhanced by using the quantum error correction, proposed by Zhou *et al.* [74], which may be a powerful tool for considering and investigating state-of-the-art quantum metrology in the future work.

ACKNOWLEDGMENTS

We sincerely thank the referees for their insightful suggestions and Dr. Jikun Xie for helpful discussions. This work was supported by the National Natural Science Foundation of China (Grants No. 11964013 and No. 11664017), the Training Program for Academic and Technical Leaders of Major Disciplines in Jiangxi Province (Grant No. 20204BCJL22053), the Postgraduate Scientific Research Innovation Project of Hunan Province (Grant No. CX20190126), and the Postgraduate Independent Exploration and Innovation Project of Central South University (Grant No. 2019zzts070).

APPENDIX A: PROOF OF THE TRANSFORMATION RELATION

For completeness, here we give the proof about the transformation relation, i.e., $\hat{S}^\dagger(\phi, 2)\hat{b}^\dagger\hat{S}(\phi, 2) = e^{-i\phi}\hat{b}^\dagger e^{-i2\phi\hat{b}^\dagger\hat{b}}$. It is well known that any operator $\hat{\zeta}$ can be expanded in Fock state space,

$$\hat{\zeta} = \sum_{m,n=0}^{\infty} \zeta_{m,n}|m\rangle\langle n|, \tag{A1}$$

where $\zeta_{m,n} = \langle m|\hat{\zeta}|n\rangle$ is the matrix element $\hat{\zeta}$ in Fock space.

Thus, if we take

$$\begin{aligned}\hat{\zeta} &= \hat{S}^\dagger(\phi, 2)\hat{b}^\dagger\hat{S}(\phi, 2)\\ &= e^{-i\phi(\hat{b}^\dagger\hat{b})^2}\hat{b}^\dagger e^{i\phi(\hat{b}^\dagger\hat{b})^2},\end{aligned} \tag{A2}$$

then the matrix element $\zeta_{m,n}$ can be calculated as

$$\zeta_{m,n} = \sqrt{n+1}e^{-i\phi(2n+1)}\delta_{m,n+1}, \tag{A3}$$

where we have used $\hat{b}^\dagger\hat{b}|n\rangle = n|n\rangle$ and $\hat{b}^\dagger|n\rangle = \sqrt{n+1}|n+1\rangle$. Substituting Eq. (A3)into Eq. (A1), we can get

$$\begin{aligned}\hat{\zeta} &= \hat{S}^\dagger(\phi, 2)\hat{b}^\dagger\hat{S}(\phi, 2)\\ &= \sum_{m,n=0}^{\infty}\sqrt{n+1}e^{-i\phi(2n+1)}\delta_{m,n+1}|m\rangle\langle n|\\ &= \sum_{n=0}^{\infty}\sqrt{n+1}e^{-i\phi(2n+1)}|n+1\rangle\langle n|\\ &= e^{-i\phi}\sum_{n=0}^{\infty}e^{-i2n\phi}\sqrt{n+1}|n+1\rangle\langle n|\\ &= e^{-i\phi}\hat{b}^\dagger e^{-i2\phi(\hat{b}^\dagger\hat{b})}.\end{aligned} \tag{A4}$$

APPENDIX B: PHASE ESTIMATION BASED ON HOMODYNE MEASUREMENT

Combining Eqs. (3) and (5), we can derive the standard deviation $\Delta\hat{X}$ as

$$\Delta\hat{X} = \sqrt{|\overline{U}|^2 + |\overline{V}|^2 + \overline{O}}, \tag{B1}$$

where we have set

$$|\overline{U}|^2 + |\overline{V}|^2 = \cosh^2 2g - \mathrm{Re}(e^{i\phi}\overline{I})\sinh^2 2g, \tag{B2}$$

and

$$\overline{O} = 2|\alpha|^2|u|^2(1 - |\overline{I}(g,\phi)|^2) + 2\mathrm{Re}(Z_1 + Z_2), \tag{B3}$$

with

$$\begin{aligned}u &= -e^{-i\phi}\sinh^2 g,\\ \chi(g,\phi) &= \frac{1}{\cosh^2 g - e^{i2\phi}\sinh^2 g},\\ \overline{I}(g,\phi) &= \chi^2(g,\phi)\exp\{|\alpha|^2[\chi(g,\phi) - 1]\},\\ Z_1 &= 2(|\alpha|^2 + \alpha^{*2})u^*\overline{I}(g,\phi)[\chi(g,\phi) - 1]\cosh^2 g,\\ Z_2 &= \alpha^2u^2\overline{I}^*(g,2\phi)[e^{-i2\phi}\chi^*(g,2\phi) - \overline{I}^*(g,2\phi)],\end{aligned} \tag{B4}$$

and the derivative of $\langle\hat{X}\rangle$

$$\partial\langle\hat{X}\rangle/\partial\phi = 2\mathrm{Re}(Z_3Z_4), \tag{B5}$$

where Re denotes the real part, and

$$\begin{aligned}Z_3 &= i\alpha^*u^*\overline{I}(g,\phi),\\ Z_4 &= 1 + 4e^{i2\phi}|u|\chi(g,\phi) + 2|\alpha|^2e^{i2\phi}|u|\chi^2(g,\phi).\end{aligned} \tag{B6}$$

Substituting Eqs. (B1) and (B5) into the error propagation formula in Eq. (6), the explicit expression of the phase sensitivity can be derived theoretically. In particular, when $\phi = 0$, we can get $|\overline{U}|^2 + |\overline{V}|^2 = 1$ and $\overline{O} = 0$. Therefore, the standard deviation $\Delta\hat{X} = 1$. Moreover, utilizing the results from Eq. (B5) at the optimal phase point $\phi = 0$, one can find the absolute value of the derivative,

$$|\partial\langle\hat{X}\rangle/\partial\phi| = \sqrt{N_\alpha}N_{\mathrm{OPA}}[1 + N_{\mathrm{OPA}}(N_\alpha + 2)]\sin\theta_\alpha. \tag{B7}$$

Then, after taking $\theta_\alpha = \frac{\pi}{2}$ leading to $\sin\theta_\alpha = 1$, we can obtain Eq. (8).

APPENDIX C: THE QFI IN THE IDEAL CASE

For a pure quantum system, the QFI can be calculated by Eq. (10), where the average value of operator $A_m = \hat{b}^{\dagger m}\hat{b}^m$ is needed [see Eq. (11)]. In order to obtain the QFI, here we use the characteristic function (CF) method. For any two-mode system, the CF is defined as

$$C_W(z_1, z_2) = \mathrm{Tr}[\rho_{\mathrm{out}}D(z_1)D(z_2)], \tag{C1}$$

where $D(z) = \exp(z\hat{a}^\dagger - z^*\hat{a})$ is the displacement operator and $\rho_{\mathrm{out}} = |\varphi_{\mathrm{out}}\rangle\langle\varphi_{\mathrm{out}}|$ is the density operator after the first

OPA. Then the expectation value $\bar{A}_m = \langle \hat{b}^{\dagger m}\hat{b}^m\rangle$ can be calculated as

$$\bar{A}_m = D_m C_N(0, z_2), \tag{C2}$$

where $C_N(0,z_2) = e^{\frac{1}{2}|z_2|^2} C_W(0,z_2)$ is the CF corresponding to normal ordering and $D_m = \frac{\partial^{2m}}{\partial z_2^m \partial(-z_2^*)^m}\ldots|_{z_2=z_2^*=0}$ is a partial differential operator. Thus one can use Eq. (C2) to calculate the expectation value $\bar{A}_m$. For our scheme, the input state $|\psi_{\rm in}\rangle = |\alpha\rangle_a \otimes |0\rangle_b$. After going through the first OPA and the phase shift, the output state is given by $|\psi_\phi\rangle = \hat{S}(\phi,k)\hat{S}(\xi_1)|\psi_{\rm in}\rangle$. Here we should note that these average values of $\bar{A}_m$ are under the state $\hat{S}(\xi_1)|\psi_{\rm in}\rangle$. Then one can obtain

$$\bar{A}_m = m!(\sinh^{2m} g) L_m(-|\alpha|^2), \tag{C3}$$

where we have utilized the relation between Laguerre polynomials and two-variable Hermit polynomials,

$$L_m(xy) = \frac{(-1)^m}{m!} H_{m,m}(x,y), \tag{C4}$$

and the generating function of $H_{m,m}(x,y)$ is

$$H_{m,m}(x,y) = \frac{\partial^{2m}}{\partial s^m \partial t^m} \exp(-st + sx + ty)|_{s=t=0}. \tag{C5}$$

Thus, substituting Eqs. (11) and (C3) into Eq. (10), one can get the explicit expression of the QFI, for the linear phase shift ($k=1$) and Kerr nonlinear phase shift ($k=2$), respectively:

$$\begin{aligned} F_1 &= 4\left(\bar{A}_2 + \bar{A}_1 - \bar{A}_1^2\right), \\ F_2 &= F_1 + f, \\ f &= 4\left[\bar{A}_4 + 6(\bar{A}_3 + \bar{A}_2) - \bar{A}_2(\bar{A}_2 + 2\bar{A}_1)\right]. \end{aligned} \tag{C6}$$

APPENDIX D: THE PHASE SENSITIVITY OF THE SU(1,1) INTERFEROMETER UNDER THE PHOTON LOSSES

Before showing the phase sensitivity of the traditional SU(1,1) interferometer in the presence of photon losses, we first derive Eq. (19). For this purpose, by using the representation of thermal entangled states [67], i.e.,

$$|\tilde{\eta}\rangle = \exp\left(-\tfrac{1}{2}|\tilde{\eta}|^2 + \tilde{\eta}\hat{b}^\dagger - \tilde{\eta}^*\hat{b}_f^\dagger + \hat{b}^\dagger\hat{b}_f^\dagger\right)|0,0_f\rangle, \tag{D1}$$

where $\hat{b}_f^\dagger$ is a fictitious mode accompanying the real photon creation operator $\hat{b}^\dagger$, $|0,0_f\rangle = |0\rangle\otimes|0_f\rangle$, and $|0_f\rangle$ is annihilated by $\hat{b}_f$ with the relations $[\hat{b}_f, \hat{b}_f^\dagger] = 1$ and $[\hat{b}, \hat{b}_f^\dagger] = 0$, one can give the formal solution of Eq. (18):

$$\begin{aligned} |\hat{\rho}\rangle = \exp[&i\tilde{\omega}\tau((\hat{b}^\dagger\hat{b})^2 - (\hat{b}_f^\dagger\hat{b}_f)^2) \\ &+ \tau(2\hat{b}\hat{b}_f - \hat{b}^\dagger\hat{b} - \hat{b}_f^\dagger\hat{b}_f)]|\hat{\rho}_0\rangle, \end{aligned} \tag{D2}$$

where $|\hat{\rho}_0\rangle = \hat{\rho}_0|\tilde{\eta}=0\rangle$. Finally, using Eq. (D2) and the operator identity [67]

$$e^{\vartheta(\hat{T}+\sigma\hat{G})} = e^{\vartheta\hat{T}}\exp[\sigma(1-e^{-\vartheta\varrho})\hat{G}/\varrho], \tag{D3}$$

which is valid for $[\hat{T},\hat{G}] = \varrho\hat{G}$, one can achieve Eq. (19).

Next, similar to the derivation of Eq. (19), the effects of photon losses on the phase sensitivity of the SU(1,1) interferometer that can also be described by the master equation

$$\frac{d\hat{\rho}}{dt} = -i\omega[\hat{b}^\dagger\hat{b},\hat{\rho}] + 2\gamma\hat{b}\rho\hat{b}^\dagger - \gamma\hat{b}^\dagger\hat{b}\hat{\rho} - \gamma\hat{\rho}\hat{b}^\dagger\hat{b}. \tag{D4}$$

According to Eq. (17), we can get

$$\frac{d\hat{\rho}}{d\tau} = i\tilde{\omega}[\hat{b}^\dagger\hat{b},\hat{\rho}] + 2\hat{b}\hat{\rho}\hat{b}^\dagger - \hat{b}^\dagger\hat{b}\hat{\rho} - \hat{\rho}\hat{b}^\dagger\hat{b}, \tag{D5}$$

and the solution for the master equation can be given by

$$\hat{\rho}(\tau) = \sum_{l=0}^{\infty}\frac{(1-e^{-2\tau})^l}{l!} e^{-(\tau-i\tilde{\omega}\tau)\hat{b}^\dagger\hat{b}}\hat{b}^l\hat{\rho}_0\hat{b}^{\dagger l}e^{-(\tau+i\tilde{\omega}\tau)\hat{b}^\dagger\hat{b}}. \tag{D6}$$

After the second OPA, the density operator of output states is then given by

$$\hat{\rho}_{\rm out}(\tau) = \hat{S}(\xi_2)\hat{\rho}(\tau)\hat{S}^\dagger(\xi_2). \tag{D7}$$

Based on the density operator $\hat{\rho}_{\rm out}(\tau)$, one can derive an analytical expression of the phase sensitivity of the SU(1,1) interferometer with the optimal point $\phi = 0$ in the presence of photon losses. Specially, for several different input states, including $|\alpha\rangle_a\otimes|0\rangle_b$ (CS&VS), $|\alpha\rangle_a\otimes|\beta\rangle_b$ (CS&CS), and $|\alpha\rangle_a\otimes|\varsigma,0\rangle_b$ (CS&SVS), we can respectively obtain the corresponding phase sensitivity as

$$\begin{aligned} \Delta\phi_{L_1(CS\&VS)} &= \frac{\sqrt{\Xi(g,\tau)-1}}{2|\alpha|e^{-\tau}\sinh^2 g}, \\ \Delta\phi_{L_1(CS\&CS)} &= \frac{\sqrt{\Xi(g,\tau)-1}}{2e^{-\tau}(|\beta|\cosh g + |\alpha|\sinh g)\sinh g}, \\ \Delta\phi_{L_1(CS\&SVS)} &= \frac{\sqrt{\Xi(g,\tau)\Gamma(r)-1}}{|\alpha|e^{-\tau}\sinh 2g}, \end{aligned} \tag{D8}$$

where $\Xi(g,\tau) = 2(\cosh^2 g - e^{-\tau}\sinh^2 g)^2$ and $\Gamma(r) = (\cosh r - \sinh r)\cosh r$.

APPENDIX E: THE PROOF OF EQS. (34) AND (35)

Using the completeness relation of the Fock state, one can get

$$\begin{aligned} \eta^{\hat{n}}\hat{n}^q\sum_{\lambda=0}^{\infty}|\lambda\rangle\langle\lambda| &= \sum_{\lambda=0}^{\infty}\eta^\lambda\lambda^q\frac{\hat{b}^{\dagger\lambda}}{\lambda!}|0\rangle\langle 0|\hat{b}^\lambda \\ &=: \sum_{\lambda=0}^{\infty}\eta^\lambda\lambda^q\frac{1}{\lambda!}\hat{b}^{\dagger\lambda}e^{-\hat{b}^\dagger\hat{b}}\hat{b}^\lambda : \\ &=: e^{-\hat{b}^\dagger\hat{b}}\sum_{\lambda=0}^{\infty}\frac{(\eta\hat{b}^\dagger\hat{b})^\lambda}{\lambda!}\frac{\partial^q}{\partial x^q}e^{x\lambda}\Big|_{x=0} : \\ &=: \frac{\partial^q}{\partial x^q}e^{(\eta e^x-1)\hat{b}^\dagger\hat{b}}\Big|_{x=0} :, \end{aligned} \tag{E1}$$

where we have used the normal ordering form of the vacuum projection operator,

$$|0\rangle\langle 0| =: e^{-\hat{b}^\dagger\hat{b}} : . \tag{E2}$$

Then, using Eq. (E1), one can calculate the following sum operator, i.e.,

$$\begin{aligned}
&\sum_{l=0}^{\infty}\frac{(1-\eta)^l}{l!}l^p\hat{b}^{\dagger l}\eta^{\hat{n}}\hat{n}^q\hat{b}^l\\
&=\sum_{l=0}^{\infty}\frac{(1-\eta)^l}{l!}l^p:(\hat{b}^\dagger\hat{b})^l\frac{\partial^q}{\partial x^q}e^{(\eta e^x-1)\hat{b}^\dagger\hat{b}}\Big|_{x=0}:\\
&=:\sum_{l=0}^{\infty}\frac{\left[(1-\eta)\hat{b}^\dagger\hat{b}\right]^l}{l!}\frac{\partial^{q+p}}{\partial x^q\partial y^p}e^{(\eta e^x-1)\hat{b}^\dagger\hat{b}+yl}\Big|_{x=y=0}:\\
&=:\frac{\partial^{q+p}}{\partial x^q\partial y^p}e^{[\eta e^x+(1-\eta)e^y-1]\hat{b}^\dagger\hat{b}}\Big|_{x=y=0}:\\
&=\frac{\partial^{q+p}}{\partial x^q\partial y^p}[\eta e^x+(1-\eta)e^y]^{\hat{b}^\dagger\hat{b}}\Big|_{x=y=0}.
\end{aligned}\tag{E3}$$

In the last step, we have used the following operator identity about $e^{\lambda\hat{b}^\dagger\hat{b}}$, i.e.,

$$e^{\lambda\hat{b}^\dagger\hat{b}}=:e^{(e^\lambda-1)\hat{b}^\dagger\hat{b}}:,\tag{E4}$$

to remove the symbol of normal ordering.

APPENDIX F: THE SPECIFIC EXPRESSION OF C_Q

Using Eqs. (29), (35), (31), and (33), one can get

$$\begin{aligned}
C_Q=&4(W_1^2\langle\Delta^2\hat{n}^2\rangle-W_2\langle\hat{n}^3\rangle+W_3\langle\hat{n}^2\rangle\\
&-W_4\langle\hat{n}\rangle-W_5\langle\hat{n}^2\rangle\langle\hat{n}\rangle-W_6\langle\hat{n}\rangle^2),
\end{aligned}\tag{F1}$$

where we have set

$$\begin{aligned}
W_1&=w_1\eta^2-2w_2\eta-\mu_2,\\
W_2&=2\eta\left(3w_1^2\eta^3-3w_3\eta^2-w_4\eta+w_5\right),\\
W_3&=\eta\left(11w_1^2\eta^3-2w_6\eta^2+w_7\eta-4w_1w_2\right),\\
W_4&=\eta(6\eta^3-12\eta^2+7\eta-1)w_1^2,\\
W_5&=2\eta(1-\eta)w_1W_1,\\
W_6&=\eta^2(1-\eta)^2w_1^2,
\end{aligned}\tag{F2}$$

as well as

$$\begin{aligned}
w_1&=1+2\mu_1-\mu_2,\\
w_2&=\mu_1-\mu_2,\\
w_3&=1+2(3\mu_1-2\mu_2)\\
&\quad+(2\mu_1-\mu_2)(4\mu_1-3\mu_2),\\
w_4&=7\mu_2-6\mu_1+24\mu_1\mu_2-14\mu_1^2-9\mu_2^2,\\
w_5&=\mu_2w_1-2w_2^2,\\
w_6&=9+40\mu_1-22\mu_2+44\mu_1^2-48\mu_1\mu_2+13\mu_2^2,\\
w_7&=7+40\mu_1-26\mu_2+52\mu_1^2-64\mu_1\mu_2+19\mu_2^2.
\end{aligned}\tag{F3}$$

In particular, when $\mu_1=\mu_2=-1$, one can obtain the expected result, i.e.,

$$F_{L_2}\leqslant C_Q=4\langle\Delta^2\hat{n}^2\rangle.\tag{F4}$$

While for $\mu_1=\mu_2=0$, corresponding to the photon losses before the Kerr nonlinear phase shift, one can get the upper bound, i.e.,

$$\begin{aligned}
F_{L_2}\leqslant C_Q=&4[\eta^4\langle\Delta^2\hat{n}^2\rangle+6\eta^3(1-\eta)\langle\hat{n}^3\rangle\\
&+\eta^2(11\eta^2-18\eta+7)\langle\hat{n}^2\rangle\\
&-\eta(6\eta^3-12\eta^2+7\eta-1)\langle\hat{n}\rangle\\
&-2\eta^3(1-\eta)\langle\hat{n}^2\rangle\langle\hat{n}\rangle-\eta^2(1-\eta)^2\langle\hat{n}\rangle^2],
\end{aligned}\tag{F5}$$

as expected.

In order to minimize C_Q, one can take $\partial C_Q/\partial\mu_1=\partial C_Q/\partial\mu_2=0$ for this purpose. Using Eqs. (F1)–(F3), it is not difficult to obtain two optimization parameters $\mu_{1\text{opt}}$ and $\mu_{2\text{opt}}$, which are, respectively, given by

$$\mu_{1\text{opt}}=\frac{BE-CD}{AD-2\eta B^2},\quad \mu_{2\text{opt}}=\frac{AE-2\eta BC}{AD-2\eta B^2},\tag{F6}$$

where we have set $A=2B_1H$, $B=B_2H$, $C=B_3H$, $D=B_4H$, and $E=\eta B_5H$. Here the column matrix H and row matrix B_j ($j=1,2,3,4,5$) are defined as the following:

$$\begin{aligned}
H&=(\langle\Delta^2\hat{n}^2\rangle,\langle\hat{n}^3\rangle,\langle\hat{n}^2\rangle,\langle\hat{n}\rangle,\langle\hat{n}^2\rangle\langle\hat{n}\rangle,\langle\hat{n}\rangle^2)^T,\\
A_1&=\eta-1,\\
A_2&=6\eta^2-6\eta+1,\\
A_3&=11\eta^2-11\eta+2,\\
A_4&=2\eta-1,\\
B_1&=(\eta A_1,-A_2,A_3,-A_2,2\eta A_1,-\eta A_1),\\
B_2&=\left(A_1^2,-3A_1A_4,A_3-A_4,-A_2,A_1A_4,-\eta A_1\right),\\
B_3&=(\eta^2,-3\eta A_4,A_3+A_4,-A_2,\eta A_4,-\eta A_1),\\
B_4&=\eta\left(\eta^{-1}A_1^3,-6A_1^2,A_3-2A_4,-A_2,2A_1^2,-\eta A_1\right),\\
B_5&=\left(\eta A_1,-A_2,A_3,-A_2,\eta^2+A_1^2,-\eta A_1\right),
\end{aligned}\tag{F7}$$

where the average value $\langle\cdot\rangle$ is in the state after the first OPA. Here we should note that only H are dependent on the input state, and the other quantities (such as A_j and B_j) are independent of the input state. If C_Q can take the minimum value, then it is also the QFI F_{L_2} of the Kerr nonlinear phase shift in the presence of photon losses. In our scheme, if we choose the states $|\psi_{\text{in}}\rangle=|\alpha\rangle_a\otimes|0\rangle_b$ as the inputs of the KSU(1,1) interferometer, then the states after the first OPA are $\hat{S}(\xi_1)|\psi_{\text{in}}\rangle$. Thus the column matrix H can be calculated as

$$\begin{aligned}
H=\Big[&\frac{F_2}{4},(\bar{A}_3+3\bar{A}_2+\bar{A}_1),\\
&(\bar{A}_2+\bar{A}_1),\bar{A}_1,\bar{A}_1(\bar{A}_2+\bar{A}_1),\bar{A}_1^2\Big]^T,
\end{aligned}\tag{F8}$$

where F_2 is a lossless result in Eq. (12) and $\bar{A}_j$ ($j=1,2,3$) and W_l ($l=1$–6) can be obtained from Eqs. (C3) and (F2), respectively.

Further substituting Eqs. (F8) and (F6) into Eq. (F1), the upper bound to the QFI $C_Q(|\alpha\rangle_a \otimes |0\rangle_b)$ in our scheme can be obtained as

$$\begin{aligned} &C_Q(|\alpha\rangle_a \otimes |0\rangle_b) \\ &\quad = W_1^2 F_2 - 4\big[W_2(\bar{A}_3 + 3\bar{A}_2 + \bar{A}_1) - W_3(\bar{A}_2 + \bar{A}_1) \\ &\qquad + W_4\bar{A}_1 + W_5\bar{A}_1(\bar{A}_2 + \bar{A}_1) + W_6\bar{A}_1^2\big], \end{aligned} \tag{F9}$$

which is just the analytical expression of the QFI. In W_l (l = 1–6), the variational parameters μ_1 and μ_2 should be replaced, respectively, by

$$\begin{aligned} \mu_{1\mathrm{opt}}(|\alpha\rangle_a \otimes |0\rangle_b) &= \frac{BE - CD}{AD - 2\eta B^2}, \\ \mu_{2\mathrm{opt}}(|\alpha\rangle_a \otimes |0\rangle_b) &= \frac{AE - 2\eta BC}{AD - 2\eta B^2}, \end{aligned} \tag{F10}$$

where $A = 2B_1H$, $B = B_2H$, $C = B_3H$, $D = B_4H$, and $E = \eta B_5 H$ with the column matrix H are shown in Eq. (F8).

In addition, for a comparison between the linear phase shift and the Kerr nonlinear one, here we give the QFI with the linear phase shift in the presence of photon losses, for several different input states, including $|\alpha\rangle_a \otimes |0\rangle_b$ (CS&VS), $|\alpha\rangle_a \otimes |\beta\rangle_b$ (CS&CS), and $|\alpha\rangle_a \otimes |\varsigma, 0\rangle_b$ (CS&SVS). In a similar way to derive Eq. (F9), for these states above together with the linear phase shift, the QFI F_{L_1} can be calculated as [72]

$$\begin{aligned} F_{L_1(CS\&VS)} &= \frac{4\eta F_1 \bar{A}_1}{(1-\eta)F_1 + 4\eta\bar{A}_1}, \\ F_{L_1(CS\&CS)} &= \frac{4\eta F_{(CS\&CS)}\langle\hat{n}\rangle_{(CS\&CS)}}{(1-\eta)F_{(CS\&CS)} + 4\eta\langle\hat{n}\rangle_{(CS\&CS)}}, \\ F_{L_1(CS\&SVS)} &= \frac{4\eta F_{(CS\&SVS)}\langle\hat{n}\rangle_{(CS\&SVS)}}{(1-\eta)F_{(CS\&SVS)} + 4\eta\langle\hat{n}\rangle_{(CS\&SVS)}}, \end{aligned} \tag{F11}$$

where $\langle\hat{n}\rangle_{(CS\&CS)}$ and $\langle\hat{n}\rangle_{(CS\&SVS)}$ are given by

$$\begin{aligned} \langle\hat{n}\rangle_{(CS\&CS)} &= (|\alpha|\sinh g + |\beta|\cosh g)^2 + \sinh^2 g, \\ \langle\hat{n}\rangle_{(CS\&SVS)} &= (|\alpha|^2 + 1)\sinh^2 g + \cosh^2 g(\sinh^2 r), \end{aligned} \tag{F12}$$

and $F_{(CS\&CS)}$ and $F_{(CS\&SVS)}$ are the lossless results which can be seen from Ref. [63], i.e.,

$$\begin{aligned} &F_{(CS\&CS)} \\ &\quad = (|\alpha|^2 + |\beta|^2)\cosh 4g + \sinh^2(2g) + 2|\alpha||\beta|\sinh 4g \\ &\qquad + |\alpha|^2 + |\beta|^2 - 2(|\alpha|^2 - |\beta|^2)\cosh 2g, \end{aligned} \tag{F13}$$

$$\begin{aligned} F_{(CS\&SVS)} = {} & \cosh^2(2g)\big[\tfrac{1}{2}\sinh^2(2r) + |\alpha|^2\big] \\ & + \sinh^2(2g)(|\alpha|^2 e^{2r} + \cosh^2 r) \\ & + |\alpha|^2(1 - 2\cosh 2g) \\ & + \tfrac{1}{4}(\cosh 4r - 1)(2\cosh 2g + 1). \end{aligned} \tag{F14}$$

[1] C. Lee, J. Huang, H. Deng, H. Dai, and J. Xu, Nonlinear quantum interferometry with Bose condensed atoms, Front. Phys. **7**, 109 (2012).

[2] J. Estève, C. Gross, A. Weller, S. Giovanazzi, and M. K. Oberthaler, Squeezing and entanglement in a Bose-Einstein condensate, Nature (London) **455**, 1216 (2008).

[3] A. C. J. Wade, J. F. Sherson, and K. Molmer, Squeezing and Entanglement of Density Oscillations in a Bose-Einstein Condensate, Phys. Rev. Lett. **115**, 060401 (2015).

[4] E. Oelker, L. Barsotti, S. Dwyer, D. Sigg, and N. Mavalvala, Squeezed light for advanced gravitational wave detectors and beyond, Opt. Express **22**, 21106 (2014).

[5] H. Vahlbruch, D. Wilken, M. Mehmet, and B. Willke, Laser Power Stabilization beyond the Shot Noise Limit Using Squeezed Light, Phys. Rev. Lett. **121**, 173601 (2018).

[6] M. Tsang, Quantum Imaging beyond the Diffraction Limit by Optical Centroid Measurements, Phys. Rev. Lett. **102**, 253601 (2009).

[7] N. Bornman, S. Prabhakar, A. Vallés, J. Leach, and A. Forbes, Ghost imaging with engineered quantum states by Hong-Ou-Mandel interference, New J. Phys. **21**, 073044 (2019).

[8] S. D. Huver, C. F. Wildfeuer, and J. P. Dowling, Entangled Fock states for robust quantum optical metrology, imaging, and sensing, Phys. Rev. A **78**, 063828 (2008).

[9] J. D. Zhang, Z. J. Zhang, L. Z. Cen, J. Y. Hu, and Y. Zhao, Nonlinear phase estimation: Parity measurement approaches the quantum Cramér-Rao bound for coherent states, Phys. Rev. A **99**, 022106 (2019).

[10] H. Liang, Y. Su, X. Xiao, Y. Che, B. C. Sanders, and X. G. Wang, Criticality in two-mode interferometers, Phys. Rev. A **102**, 013722 (2020).

[11] S. Ataman, Optimal Mach-Zehnder phase sensitivity with Gaussian states, Phys. Rev. A **100**, 063821 (2019).

[12] C. P. Wei, Z. M. Wu, C. Z. Deng, and L. Y. Hu, Phase sensitivity of a three-mode nonlinear interferometer, Opt. Commun. **452**, 189 (2019).

[13] J. Joo, W. J. Munro, and T. P. Spiller, Quantum Metrology with Entangled Coherent States, Phys. Rev. Lett. **107**, 083601 (2011).

[14] R. Birrittella and C. C. Gerry, Quantum optical interferometry via the mixing of coherent and photon-subtracted squeezed vacuum states of light, J. Opt. Soc. Am. B **31**, 586 (2014).

[15] J. P. Dowling, Quantum optical metrology—the lowdown on high-N00N states, Contemp. Phys. **49**, 125 (2008).

[16] L. Y. Hu, C. P. Wei, J. H. Huang, and C. J. Liu, Quantum metrology with Fock and even coherent states: Parity detection approaches to the Heisenberg limit, Opt. Commun. **323**, 68 (2014).

[17] J. Kong, Z. Y. Ou, and W. P. Zhang, Phase-measurement sensitivity beyond the standard quantum limit in an interferometer consisting of a parametric amplifier and a beam splitter, Phys. Rev. A **87**, 023825 (2013).

[18] Z. Y. Ou, Enhancement of the phase-measurement sensitivity beyond the standard quantum limit by a nonlinear interferometer, Phys. Rev. A **85**, 023815 (2012).

[19] S. H. Tan, Y. Y. Gao, H. de Guise, and B. C. Sanders, SU(3) Quantum Interferometry with Single-Photon Input Pulses, Phys. Rev. Lett. **110**, 113603 (2013).

[20] B. Yurke, S. L. McCall, and J. R. Klauder, SU(2) and SU(1,1) interferometers, Phys. Rev. A **33**, 4033 (1986).

[21] H. M. Ma, D. Li, C. H. Yuan, L. Q. Chen, Z. Y. Ou, and W. P. Zhang, SU(1,1)-type light-atom-correlated interferometer, Phys. Rev. A **92**, 023847 (2015).

[22] E. Distante, M. Ježek, and U. L. Andersen, Deterministic Superresolution with Coherent States at the Shot Noise Limit, Phys. Rev. Lett. **111**, 033603 (2013).

[23] X. M. Feng, G. R. Jin, and W. Yang, Quantum interferometry with binary-outcome measurements in the presence of phase diffusion, Phys. Rev. A **90**, 013807 (2014).

[24] R. A. Campos, C. C. Gerry, and A. Benmoussa, Optical interferometry at the Heisenberg limit with twin Fock states and parity measurements, Phys. Rev. A **68**, 023810 (2003).

[25] Y. Israel, S. Rosen, and Y. Silberberg, Supersensitive Polarization Microscopy Using NOON States of Light, Phys. Rev. Lett. **112**, 103604 (2014).

[26] C. M. Caves, Quantum-mechanical noise in an interferometer, Phys. Rev. D **23**, 1693 (1981).

[27] P. M. Anisimov, G. M. Raterman, A. Chiruvelli, W. N. Plick, S. D. Huver, H. Lee, and J. P. Dowling, Quantum Metrology with Two-Mode Squeezed Vacuum: Parity Detection Beats the Heisenberg Limit, Phys. Rev. Lett. **104**, 103602 (2010).

[28] J. Fiurášek, Conditional generation of N-photon entangled states of light, Phys. Rev. A **65**, 053818 (2002).

[29] A. Ourjoumtsev, H. Jeong, R. Tualle-Brouri, and P. Grangier, Generation of optical 'Schrödinger cats' from photon number states, Nature (London) **448**, 784 (2007).

[30] T. Ono and H. F. Hofmann, Effects of photon losses on phase estimation near the Heisenberg limit using coherent light and squeezed vacuum, Phys. Rev. A **81**, 033819 (2010).

[31] D. Li, C. H. Yuan, Z. Y. Ou, and W. P. Zhang, The phase sensitivity of an SU(1,1) interferometer with coherent and squeezed-vacuum light, New J. Phys. **16**, 073020 (2014).

[32] X. Y. Hu, C. P. Wei, Y. F. Yu, and Z. M. Zhang, Enhanced phase sensitivity of an SU(1,1) interferometer with displaced squeezed vacuum light, Front. Phys. **11**, 114203 (2016).

[33] W. N. Plick, J. P. Dowling, and G. S. Agarwal, Coherent-light-boosted, sub-shot noise, quantum interferometry, New J. Phys. **12**, 083014 (2010).

[34] L. L. Guo, Y. F. Yu, and Z. M. Zhang, Improving the phase sensitivity of an SU(1,1) interferometer with photon-added squeezed vacuum light, Opt. Express **26**, 29099 (2018).

[35] D. Li, B. T. Gard, Y. Gao, C. H. Yuan, W. P. Zhang, H. Lee, and J. P. Dowling, Phase sensitivity at the Heisenberg limit in an SU(1,1) interferometer via parity detection, Phys. Rev. A **94**, 063840 (2016).

[36] S. Adhikari, N. Bhusal, C. You, H. Lee, and J. P. Dowling, Phase estimation in an SU(1,1) interferometer with displaced squeezed states, Opt. Express **1**, 438 (2018).

[37] C. Sparaciari, S. Olivares, and M. G. A. Paris, Gaussian-state interferometry with passive and active elements, Phys. Rev. A **93**, 023810 (2016).

[38] F. Hudelist, J. Kong, C. J. Liu, J. T. Jing, Z. Y. Ou, and W. P. Zhang, Quantum metrology with parametric amplifier-based photon correlation interferometers, Nat. Commun. **5**, 3049 (2014).

[39] G. F. Jiao, K. Y. Zhang, L. Q. Chen, W. P. Zhang, and C. H. Yuan, Nonlinear phase estimation enhanced by an actively correlated Mach-Zehnder interferometer, Phys. Rev. A **102**, 033520 (2020).

[40] O. Seth, X. F. Li, H. N. Xiong, J. Y. Luo, and Y. X. Huang, Improving the phase sensitivity of an SU(1,1) interferometer via a nonlinear phase encoding, J. Phys. B: At. Mol. Opt. Phys. **53**, 205503 (2020).

[41] S. K. Chang, C. P. Wei, H. Zhang, Y. Xia, W. Ye, and L. Y. Hu, Enhanced phase sensitivity with a nonconventional interferometer and nonlinear phase shifter, Phys. Lett. A **384**, 126755 (2020).

[42] C. P. Wei and Z. M. Zhang, Improving the phase sensitivity of a Mach-Zehnder interferometer via a nonlinear phase shifter, J. Mod. Opt. **64**, 743 (2017).

[43] Z. Tong, C. Lundström, P. A. Andrekson, C. J. Mckinstrie, M. Karlsson, D. J. Blessing, E. Tipsuwannakul, B. J. Puttnam, H. Toda, and L. Grüernielsen, Towards ultrasensitive optical links enabled by low-noise phase-sensitive amplifiers, Nat. Photonics **5**, 430 (2011).

[44] N. V. Corzo, A. M. Marino, K. M. Jones, and P. D. Lett, Noiseless Optical Amplifier Operating on Hundreds of Spatial Modes, Phys. Rev. Lett. **109**, 043602 (2012).

[45] J. Joo, K. Park, H. Jeong, W. J. Munro, K. Nemoto, and T. P. Spiller, Quantum metrology for nonlinear phase shifts with entangled coherent states, Phys. Rev. A **86**, 043828 (2012).

[46] L. Dong, J. X. Wang, Q. Y. Li, H. Z. Shen, H. K. Dong, X. M. Xiu, Y. J. Gao, and C. H. Oh, Nearly deterministic preparation of the perfect W state with weak cross-Kerr nonlinearities, Phys. Rev. A **93**, 012308 (2016).

[47] S. Ataman, Phase sensitivity of a Mach-Zehnder interferometer with single-intensity and difference-intensity detection, Phys. Rev. A **98**, 043856 (2018).

[48] X. Xiao, H. B. Liang, G. L. Li, and X. G. Wang, Enhancement of sensitivity by initial phase matching in SU(1,1) interferometers, Commun. Theor. Phys. **71**, 037 (2019).

[49] X. X. Jing, J. Liu, W. Zhong, and X. G. Wang, Quantum fisher information of entangled coherent states in a lossy mach-zehnder interferometer, Commun. Theor. Phys. **61**, 115 (2014).

[50] H. Zhang, W. Ye, C. P. Wei, Y. Xia, S. K. Chang, Z. Y. Liao, and L. Y. Hu, Improved phase sensitivity in a quantum optical interferometer based on multiphoton catalytic two-mode squeezed vacuum states, Phys. Rev. A **103**, 013705 (2021).

[51] K. P. Seshadreesan, S. Kim, J. P. Dowling, and H. Lee, Phase estimation at the quantum Cramér-Rao bound via parity detection, Phys. Rev. A **87**, 043833 (2013).

[52] W. Ye, H. Zhong, Q. Liao, D. Huang, L. Y. Hu, and Y. Guo, Improvement of self-referenced continuous-variable quantum key distribution with quantum photon catalysis, Opt. Express **27**, 17186 (2019).

[53] L. Y. Hu, M. Al-amri, Z. Y. Liao, and M. S. Zubairy, Continuous-variable quantum key distribution with non-Gaussian operations, Phys. Rev. A **102**, 012608 (2020).

[54] Y. Guo, W. Ye, H. Zhong, and Q. Liao, Continuous-variable quantum key distribution with non-Gaussian quantum catalysis, Phys. Rev. A **99**, 032327 (2019).

[55] S. L. Braunsteina and P. V. Loock, Quantum information with continuous variables, Rev. Mod. Phys. **77**, 513 (2005).

[56] W. Ye, Y. Guo, Y. Xia, H. Zhong, H. Zhang, J. Z. Ding, and L. Y. Hu, Discrete modulation continuous-variable quantum key

distribution based on quantum catalysis, Acta Phys. Sin. **69**, 060301 (2020).

[57] J. Cheng, Quantum metrology for simultaneously estimating the linear and nonlinear phase shifts, Phys. Rev. A **90**, 063838 (2014).

[58] A. Luis, Quantum limits, nonseparable transformations, and nonlinear optics, Phys. Rev. A **76**, 035801 (2007).

[59] S. Boixo, A. Datta, S. T. Flammia, A. Shaji, E. Bagan, and C. M. Caves, Quantum-limited metrology with product states, Phys. Rev. A **77**, 012317 (2008).

[60] S. Boixo, A. Datta, M. J. Davis, S. T. Flammia, A. Shaji, and C. M. Caves, Quantum Metrology: Dynamics versus Entanglement, Phys. Rev. Lett. **101**, 040403 (2008).

[61] M. Napolitano and M. W. Mitchell, Nonlinear metrology with a quantum interface, New J. Phys. **12**, 093016 (2010).

[62] M. Zwierz, C. A. Pérez-Delgado, and P. Kok, General Optimality of the Heisenberg Limit for Quantum Metrology, Phys. Rev. Lett. **105**, 180402 (2010).

[63] Q. K. Gong, D. Li, C. H. Yuan, Z. Y. Qu, and W. P. Zhang, Phase estimation of phase shifts in two arms for an SU(1,1) interferometer with coherent and squeezed vacuum states, Chin. Phys. B **26**, 094205 (2017).

[64] D. Li, C. H. Yuan, Y. Yao, W. Jiang, M. Li, and W. P. Zhang, Effects of loss on the phase sensitivity with parity detection in an SU(1,1) interferometer, J. Opt. Soc. Am. B **35**, 1080 (2018).

[65] R. Demkowicz-Dobrzański, M. Jarzyna, and J. Kołodyński, Quantum limits in optical interferometry, Prog. Opt. **60**, 345 (2015).

[66] C. C. Gerry, A. Benmoussa, and R. A. Campos, Nonlinear interferometer as a resource for maximally entangled photonic states: Application to interferometry, Phys. Rev. A **66**, 013804 (2002).

[67] L. Y. Hu, F. Chen, Z. S. Wang, and H. Y. Fan, Time evolution of distribution functions in dissipative environments, Chin. Phys. B **20**, 074204 (2011).

[68] S. Knysh, V. N. Smelyanskiy, and G. A. Durkin, Scaling laws for precision in quantum interferometry and the bifurcation landscape of the optimal state, Phys. Rev. A **83**, 021804(R) (2011).

[69] J. Liu, X. X. Jing, and X. G. Wang, Phase-matching condition for enhancement of phase sensitivity in quantum metrology, Phys. Rev. A **88**, 042316 (2013).

[70] Matteo A. C. Rossi, F. Albarelli, and M. G. A. Paris, Enhanced estimation of loss in the presence of Kerr nonlinearity, Phys. Rev. A **93**, 053805 (2016).

[71] Marco G. Genoni, C. Invernizzi, and Matteo G. A. Paris, Enhancement of parameter estimation by Kerr interaction, Phys. Rev. A **80**, 033842 (2009).

[72] B. M. Escher, R. L. de Matos Filho, and L. Davidovich, General framework for estimating the ultimate precision limit in noisy quantum-enhanced metrology, Nat. Phys. **7**, 406 (2011).

[73] H. Y. Fan, H. L. Lu, and Y. Fan, Newton-Leibniz integration for ket-bra operators in quantum mechanics and derivation of entangled state representations, Ann. Phys. **321**, 480 (2006).

[74] S. S. Zhou, M. Z. Zhang, J. Preskill, and L. Jiang, Achieving the Heisenberg limit in quantum metrology using quantum error correction, Nat. Commun. **9**, 78 (2018).